Efficient optimum seismic design of reinforced concrete frames with nonlinear structural analysis procedures

Panagiotis E. Mergos *

Research Centre for Civil Engineering Structures, Department of Civil Engineering,
City, University of London, London EC1V 0HB, UK

Abstract. Performance-based seismic design offers enhanced control of structural damage for different levels of earthquake hazard. Nevertheless, the number of studies dealing with the optimum performance-based seismic design of reinforced concrete frames is rather limited. This observation can be attributed to the need for nonlinear structural analysis procedures to calculate seismic demands. Nonlinear analysis of reinforced concrete frames is accompanied by high computational costs and requires *a priori* knowledge of steel reinforcement. To address this issue, previous studies on optimum performance-based seismic design of reinforced concrete frames use independent design variables to represent steel reinforcement in the optimization problem. This approach drives to a great number of design variables, which magnifies exponentially the search space undermining the ability of the optimization algorithms to reach the optimum solutions. This study presents a computationally efficient procedure tailored to the optimum performance-based seismic design of reinforced concrete frames. The novel feature of the proposed approach is that it employs a deformation-based, iterative procedure for the design of steel reinforcement of reinforced concrete frames to meet their performance objectives given the cross-sectional dimensions of the structural members. In this manner, only the cross-sectional dimensions of structural members need to be addressed by the optimization algorithms as independent design variables. The developed solution strategy is applied to the optimum seismic design of reinforced concrete frames using pushover and nonlinear response-history analysis and it is found that it outperforms previous solution approaches.

Keywords: Reinforced concrete; seismic design; performance-based; structural optimization; computationally efficient; nonlinear structural analysis; genetic algorithms

1 Introduction

The need for enhanced control of damage of structural systems subjected to earthquake ground motions has led to the development of deformation- and performance-based seismic design methodologies. Deformation-based seismic design offers direct control of structural damage that is related to member deformations (Priestley *et al*. 2007, Fardis 2009). Several deformation-based seismic design methodologies (e.g. Priestley *et al*. 2007, Panagiotakos & Fardis 2001, Kappos & Stefanidou 2010) have been presented in the literature and an interesting comparative study of them can be found in (*fib* 2003). Furthermore, performance-based seismic design offers advanced control of structural damage by requiring a set of

* Corresponding author. Panagiotis E. Mergos, Lecturer in Structural Engineering, Department of Civil Engineering, City University London, EC1V 0HB, London, UK.
E-mail address: panagiotis.mergos.1@city.ac.uk, Tel. 0044 (0) 207040 8417

performance objectives, in terms of structural damage, to be met for different levels of seismic hazard (SEAOC 2000). Performance- and deformation-based seismic design is now widely acknowledged and adopted in modern seismic design guidelines such as the one included in the *fib* Model Code 2010 (*fib* 2010, Fardis 2013) that is meant to serve as a basis for future design codes of concrete structures.

A basic prerequisite of reliable performance-based seismic design is the accurate calculation of seismic demands in terms of both member deformations and forces. To serve this goal, nonlinear structural analysis procedures are required that are able to reproduce inelastic response of structural systems subjected to strong ground motions. The most rigorous method for calculating inelastic seismic demands is the nonlinear response-history analysis with step-by-step integration of the equation of motion in the time domain. Alternatively, pushover analysis can be used to avoid the complexity and computational effort of nonlinear response-history analysis. However, this analysis procedure exhibits several limitations, mainly related to its inability to account for higher mode effects (Krawinkler 1996). Therefore, it is generally recommended for regular frames with no significant higher mode effects (Krawinkler 1996, CEN 2004).

Efficient design should not only control the level of structural damage but also lead to sustainable structural solutions in terms of both economic cost and environmental impact (Mergos 2018). The demand for sustainable structural design solutions in limited time has driven to the development of automated optimum structural design methodologies making use of efficient optimization algorithms that are able to solve complex engineering problems in limited time (Yang 2014, Lagaros 2014).

Extensive research has been conducted on automated optimum design of structural systems (Lagaros 2014). However, only a limited number of studies has focussed on deformation- and performance-based seismic design of reinforced concrete frames with the aid of nonlinear structural analysis procedures (Fragiadakis & Lagaros 2011, Lagaros 2014). A list of these studies is presented in the following. Clearly, this list is not intended to be exhaustive but simply to provide a brief overview of the design variables, objective functions and constraints as well as the structural analysis procedures used in these research efforts.

Ganzerli *et al*. (2000) were the first to consider optimum seismic design with performance-based constraints of a simple reinforced concrete portal frame. Performance constraints were expressed in terms of member ends plastic rotations following FEMA-273 guidelines (FEMA 1997). Seismic demands were evaluated using pushover analysis. Material cost was selected as the single design objective. Cross-sectional dimensions and longitudinal reinforcing steel areas were set as the design variables. Transverse reinforcement was not considered as it was expected not to appreciably change the outcome of the optimum solution. Chan and Zou (2004) used optimality criteria approach to examine optimum seismic design of reinforced concrete frames using pushover analysis. The proposed methodology is divided in two steps. First, member section dimensions are selected to fulfill the Serviceability Limit State (SLS) for frequent earthquakes. Next, member longitudinal steel reinforcement is designed to withstand demands of rare earthquakes for the Ultimate Limit State (ULS). This approach has the advantage of splitting the optimization problem into two smaller-scale optimization tasks that can be more easily resolved. However, it does not consider the fact that the response of reinforced concrete frames, even at the SLS, is a function of the existing longitudinal steel reinforcement (Priestley *et al*. 2007, Fardis 2009). Fragiadakis and Papadrakakis (2008) developed a performance-based optimum seismic design methodology for reinforced concrete frames using nonlinear response-history analysis and following both a deterministic and reliability-based approach. Inter-story drifts were used as performance criteria and material cost was set as the design objective to be minimized. Design variables were determined by using tables of concrete sections with pre-determined longitudinal steel reinforcement and

applying the concept of multi-database cascade optimization. Lagaros and Fragiadakis (2011) compared optimum performance-based seismic designs of reinforced concrete buildings by using three different pushover methods. Cross-sectional dimensions and longitudinal steel reinforcement are used as design variables. The expected life cycle cost is set as design objective that consists of the initial construction cost and the limit state cost accounting for the costs related to damages induced by earthquakes during the lifetime of the structures. Gencturk (2013) examined performance-based seismic design optimization of reinforced concrete and reinforced engineered cementitious composites (ECC) frames. Initial cost and seismic performance, in terms of inter-storey drifts for the 10/50 hazard level, are set as the design objectives. Cross-sectional dimensions and longitudinal steel reinforcement ratios are used as design variables. Transverse reinforcement of the reinforced concrete frames is evaluated based on ACI 318-08 (ACI 2008) guidelines and it is included in the calculation of the initial cost of the design solutions. Mergos (2017) compared optimum seismic designs of reinforced concrete frames designed according to the deformation- and performance-based design methodology of *fib* Model Code 2010 (*fib* 2010) and the prescriptive approach of Eurocode 8 – Part 1 (CEN 2004). In this study, material cost is set as the design objective and cross-sectional dimensions, longitudinal and transversal reinforcing steel properties are used as design variables. Nonlinear response-history analysis is used to calculate seismic demands. It is found that the *fib* Model Code (MC2010) approach drives to significant cost savings, especially in regions of low seismicity, and controls better the levels of seismic damage.

It can be inferred from this literature review that previous studies dealing with the optimum performance-based seismic design of reinforced concrete structures include the steel reinforcement (typically the longitudinal reinforcement) in the form of independent design variables in the optimization problem. This approach increases greatly the number of design variables expanding exponentially the search space and undermining the efficiency of the optimization algorithms to track the optimum solutions. The problem is magnified by the high computational costs needed to conduct nonlinear seismic analyses that turn, in many cases, the time required to perform optimum performance-based seismic design of reinforced frames prohibitive.

In this study, a new methodology for the computationally efficient performance-based seismic design of reinforced concrete frames using nonlinear structural analysis procedures is developed. The novel feature of the proposed approach is that it employs a simple, deformation-based, iterative procedure for the design of steel reinforcement of reinforced concrete frames to meet their performance objectives given the cross-sectional dimensions of their structural members. In this manner, only the cross-sectional dimensions of structural members need to be set as independent design variables reducing greatly the search space of the optimization problem and facilitating the optimization algorithms to reach the optimum solutions. In the following, the proposed methodology is first developed. Next, it is applied to different reinforced concrete frames and it is compared with the performance of a more standard approach using steel reinforcement bars as independent design variables.

2 Optimum seismic design of reinforced concrete frames methodology

2.1 Optimization problem formulation

Optimum seismic design of reinforced concrete frames can be formulated as a standard optimization problem with discrete design variables. This is the case because the design

variables (i.e. cross-sectional dimensions, steel reinforcement bars) can take only pre-determined discrete values specified by construction industry. A single-objective optimization problem with discrete design variables is generally written as:

$$\begin{aligned} &\text{Minimize:} && \mathrm{F}(\boldsymbol{x}) \\ &\text{Subject to:} && g_j(\boldsymbol{x}) \leq 0,\ j = 1\ to\ m \\ &\text{Where:} \\ & && \boldsymbol{x} = (x_1, x_2, \dots, x_n) \\ & && x_i \in D_i = \left(d_{i1}, d_{i2}, \dots, d_{ik_i}\right), i = 1\ to\ n \end{aligned} \qquad (1)$$

In this formulation, $\mathrm{F}(\boldsymbol{x})$ represents the objective function to be minimized by the optimization problem. The vector $\boldsymbol{x}$ is the candidate design solution that contains n independent design variables x_i (i =1 to n). Design variables x_i take values from discrete sets of values $\boldsymbol{D}_i = (d_{i1}, d_{i2}, \dots, d_{iki})$, where d_{ip} (p = 1 to k_i) is the p-th possible discrete value of design variable x_i and k_i is the number of possible discrete values of x_i. Furthermore, the solution should be subject to m number of constraints $g_j(\boldsymbol{x}) \leq 0$ (j = 1 to m). The objective function, design variables and design constraints as well as the solution strategies and algorithms used in this study to solve the optimization problem of Eq. (1) are discussed in detail in the subsequent sections.

2.2 Objective function

The objective function $\mathrm{F}(\boldsymbol{x})$ addressed in this study is the material cost of reinforced concrete frames. This cost can be taken as the sum of costs of concrete $C_c(\boldsymbol{x})$, steel $C_s(\boldsymbol{x})$ and formworks $C_f(\boldsymbol{x})$. The cost of concrete is taken equal to the product of total concrete volume V_c (m^3) times the cost of concrete per unit volume C_{co} (€ / m^3). The cost of steel is calculated by multiplying the total mass of steel reinforcement m_s (kg) by the cost of steel per unit mass C_{so} (€ / kg). The cost of formworks is found as the product of the total area A_f (m^2) of formworks times their cost per unit area C_{fo} (€ / m^2). V_c, m_s and A_f are calculated by summing up the contributions of all beams and columns of the concrete frames. The following unit prices are assumed in the rest of this study: C_{co} = 100 € / m^3, C_{so} = 1 € / kg and C_{fo} = 15 € / m^2.

2.3 Design parameters and variables

In optimum design problems, the input data can be divided in design parameters that keep their values fixed during the optimization process and design variables. In the sizing optimization problem examined herein, design parameters are assumed the geometry, material properties, concrete cover and external loading of the reinforced concrete frames. On the other hand, design variables determine dimensions and steel reinforcement of section properties. Design variables are grouped in sub-vectors that they form the design vector $\boldsymbol{x}$ by assembly as described in the following.

Column section properties design variable sub-vectors are the heights $\boldsymbol{h_c}$ and widths $\boldsymbol{b_c}$ of the rectangular column sections, the diameters $\boldsymbol{d_{bc}}$ and numbers $\boldsymbol{n_c}$ of main bars per side, assumed herein the same for all sides of a section for simplicity, the diameters $\boldsymbol{d_{bwc}}$, spacings $\boldsymbol{s_c}$ and numbers of legs $\boldsymbol{n_{wc}}$ of transverse reinforcement assumed again the same in both directions of a section for simplification purposes (Fig. 1a). Beam section properties design variable sub-vectors are the heights $\boldsymbol{h_b}$ and widths $\boldsymbol{b_b}$ of the beam sections, the diameters $\boldsymbol{d_{bt}}$ and numbers of main bars $\boldsymbol{n_{tb}}$ at the top, the diameters $\boldsymbol{d_{bb}}$ and numbers $\boldsymbol{n_{bb}}$ of main bars at the bottom, the diameters $\boldsymbol{d_{bwb}}$, spacings $\boldsymbol{s_b}$ and numbers of legs $\boldsymbol{n_{wb}}$ of transverse reinforcement parallel to beam section heights (Fig. 1b).

It can be easily deducted that the design variables can be further grouped in three distinct compound design sub-vectors. The cross-sectional dimensions sub-vector $\boldsymbol{x_{cd}} = [\boldsymbol{h_c}, \boldsymbol{b_c}, \boldsymbol{h_b}, \boldsymbol{b_b}]$, the longitudinal steel reinforcement bars sub-vector $\boldsymbol{x_{sl}} = [\boldsymbol{d_{bc}}, \boldsymbol{n_c}, \boldsymbol{d_{bt}}, \boldsymbol{n_{tb}}, \boldsymbol{d_{bb}}, \boldsymbol{n_{bb}}]$ and the transverse steel reinforcement bars sub-vector $\boldsymbol{x_{sw}} = [\boldsymbol{d_{bwc}}, \boldsymbol{n_{wc}}, \boldsymbol{s_c}, \boldsymbol{d_{bwb}}, \boldsymbol{n_{wb}}, \boldsymbol{s_b}]$. These three sub-vectors can be assembled to form the design vector $\boldsymbol{x} = [\boldsymbol{x_{cd}}, \boldsymbol{x_{sl}}, \boldsymbol{x_{sw}}]$.

Having established section properties, member properties need to be defined. These include both design parameters like member lengths, material properties and concrete cover as well as section properties. Two section properties per member property are used in this study representing member end sections. It is assumed that seismic demands control the structural design of the examined frames and therefore member end sections are the critical locations of the structural members. Furthermore, for simplicity, it is assumed that the end section properties are used throughout the corresponding half member lengths. Further cost reductions are feasible by optimizing the supplied steel reinforcement along member lengths. However, this should also take into account the ease of construction and it is not expected to alter the main findings of this study.

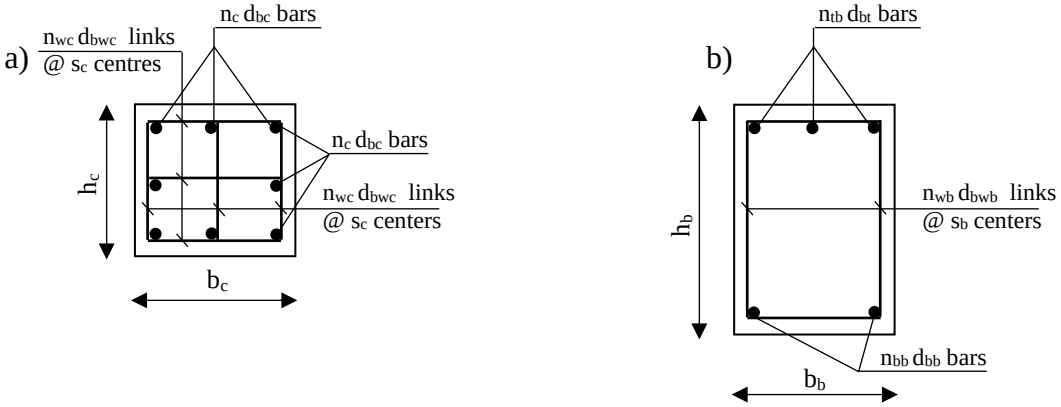

Fig. 1: Design variables: a) column sections; b) beam sections

2.4 Design constraints

The design constraints of the optimization problem examined herein are mainly related to the deformation- and performance-based seismic design methodology adopted in MC2010 (*fib* 2010). However, prior to the seismic design provisions, construction practice constraints and constraints referring to structural design for static loads must be addressed. In this study, design constraints for static loads are based on the provisions of Eurocode 2 (EC2) (CEN 2000). EC2 design constraints are either related to Engineering Demand Parameters (*EDP*) (i.e. forces, displacements, drifts, etc.) or Structural Detailing Parameters (*SDP*). A detailed description of these constraints and how they can be expressed in the generic form $g_j(\boldsymbol{x}) \leq 0$ of Eq. (1) can be found in (Mergos 2017).

MC2010 adopts a fully-fledged, performance-based seismic design methodology (Fardis 2013). The code requires the verification of 4 Limit States. The Operational (OP) and Immediate Use (IU) which are SLS and the Life Safety (LS) and Collapse Prevention (CP) which represent ULS. All Limit States are verified by comparing chord rotation demands θ_{Ed}, for different levels of Seismic Hazard, with chord rotation limit values θ_{lim} as presented in Table 1.

In Table 1, θ_y is the yield chord rotation of concrete members. For beams and rectangular columns with ribbed bars, θ_y is given by Eq. (2), where φ_y is the end section yield curvature, L_s the shear span of the member on the side of the end section, z is the lever arm of the end

section, a_{scr} is a coefficient equal to 1 if shear cracking precedes flexural yielding or equal to 0 if not, h is the end section height, d_{bl} and f_{yl} are the diameter and yield strength of longitudinal reinforcement (MPa) and f_c the concrete strength of the member in MPa. It is interesting to observe in this equation that θ_y is independent of the transverse reinforcement (Priestley *et al*. 2007, Fardis 2009).

$$\theta_y = \frac{\varphi_y(Ls+a_{scr}\cdot z)}{3} + 0.0014\cdot\left(1+\frac{1.5h}{L_s}\right) + \frac{\varphi_y d_{bL} f_{yl}}{8\sqrt{f_c}} \qquad (2)$$

Furthermore, $\theta^{pl}{}_{u,k}$ is the characteristic ultimate plastic hinge rotation capacity derived by the respective mean value $\theta^{pl}{}_{um}$ divided by the partial safety factor γ_{Rd}. For rectangular beams and columns with ductile steel reinforcement and without diagonal reinforcement, γ_{Rd} can be taken equal to 1.75 if $\theta^{pl}{}_{u,m}$ is calculated by Eq. (3). In this equation, ω_1 and ω_2 are the mechanical ratios of reinforcement in tension and compression zone respectively, v is the normalized axial load ratio, a is the confinement effectiveness factor and $\rho_w$and $f_{yw}$are the volumetric ratio and yield strength of transverse reinforcement. It is evident in this equation that $\theta^{pl}{}_{um}$ strongly depends on the transverse reinforcement. Therefore, the latter should be adjusted accordingly so that the ULS are satisfied.

$$\theta_{um}^{pl} = 0.0143\cdot 0.25^{v}\cdot f_c^{0.2}\cdot\left(\frac{\max(0.01;\omega_2)}{\max(0.01;\omega_1)}\right)^{0.3}\cdot\left(\min\left(9;\frac{L_s}{h}\right)\right)^{0.35}\cdot 25^{\left(\frac{a\rho_w f_{yw}}{f_c}\right)} \qquad (3)$$

Furthermore, for the ULS, brittle shear failures should be prevented by ensuring that shear force demands V_{Ed} are lesser than design shear force limit values (capacities) $V_{lim} = V_{Rd}$. V_{Rd} values outside plastic hinge regions are calculated as for static loadings. Inside plastic hinge regions, *fib* MC2010 specifies a strut inclination of 45° when plastic rotation θ^{pl} exceeds $2\cdot\theta_y$ and 21.8° for elastic response. Interpolation is allowed for intermediate values of θ^{pl}.

Conveniently, all MC2010 performance-based constraints can be expressed in the generic form $g_j(\boldsymbol{x}) \leq 0$ by Eq. (4), where *EDPs* represent chord rotations and shear forces. It is also important to clarify herein that MC2010 follows a purely performance-based approach and no additional prescriptive rules (i.e. detailing rules, capacity design principles) are set to meet its performance objectives apart from the ones used for static loads.

$$EDP \leq EDP_{lim} \rightarrow g_j(x) = \frac{EDP}{EDP_{lim}} - 1 \leq 0 \ (j = 1\ to\ m) \qquad (4)$$

Seismic demands according to *fib* MC2010 should be calculated by rigorous nonlinear structural analysis employing lumped plasticity finite elements with bilinear moment-rotation hysteretic models and realistic rules for stiffness degradation during unloading and reloading. Furthermore, the finite element model applied should use realistic estimates of the effective elastic stiffness of concrete members EI_{eff}. It is therefore recommended that EI_{eff} is taken from Eq. (5), where M_y represents the member end section yield moments and the other parameters have been previously defined. It is important to identify here that EI_{eff} is directly proportional to member's flexural strength that is strongly influenced by the amount of longitudinal steel reinforcement. Therefore, calculation of seismic demands requires the knowledge of longitudinal steel reinforcement even at the SLS.

$$EI_{eff} = \frac{M_y L_s}{3\theta_y} \qquad (5)$$

The one-component lumped plasticity finite element (Giberson, 1967) is used in this study for calculating seismic demands. This is a series model of an elastic element and two nonlinear rotational springs at its ends, where all inelastic deformations are lumped. Hysteretic rules representative of well-detailed and flexure-controlled reinforced concrete members are used since this study is focussing on the design of new structures. More particularly, mild stiffness degradation during unloading is considered following the recommendations by Sivaselvan and Reinhorn (2000) and Mergos and Kappos (2012). Furthermore, it is assumed that reloading aims at the point of previous maximum excursion in the opposite direction (Filippou *et al*. 1992, Mergos and Kappos 2012). For simplicity, a fixed post-yield hardening ratio close to zero (elastic-perfectly plastic behaviour) is assumed for the bilinear moment-rotation hysteretic models following the recommendations by Fardis (2013).

Table 1: Limit States, Seismic Hazard levels and Deformation Limits recommended by *fib* MC2010 for ordinary structures

Limit State	**Seismic Hazard**	**Deformation Limits θ_{lim}**
Operational (OP)	Frequent with 70% probability of exceedance in 50 years (70/50)	Mean value of θ_y
Immediate Use (IU)	Occasional with 40% probability of exceedance in 50 years (40/50)	Mean value of θ_y may be exceeded by a factor of 2.0
Life Safety (LS)	Rare with 10% probability of exceedance in 50 years (10/50)	Safety factor γ^*_R of 1.35 against ${\theta^{pl}}_{u,k}$
Collapse Prevention (CP)	Very rare with 2% probability of exceedance in 50 years (2/50)	${\theta^{pl}}_{u,k}$ capacity may be reached (γ^*_R =1)

2.5 Solution strategies

In this section, the strategies followed to solve the afore-described optimization problem are presented. The first strategy (Fig. 2a) examined herein is named for simplicity "standard" because it is more representative of previous studies on optimum performance-based seismic design of reinforced concrete structures, where both the cross-sectional dimensions and the longitudinal reinforcement of concrete members are set as design variables (e.g. Ganzerli *et al*. 2000, Fragiadakis and Papadrakakis 2008, Gencturk 2013, Mergos 2017). It is emphasised, however, that the 'standard' approach examined in this study by no means represents fully the special characteristics of specific previous studies and such comparisons are not implied herein.

In this strategy, the optimizer selects the $\boldsymbol{x_{cd}}$ and $\boldsymbol{x_{sl}}$ design sub-vectors. The candidate designs are first checked to verify that they comply with construction practice and detailing rules for static loads limitations (e.g. the width of beams cannot be greater than the width of adjoining columns, maximum longitudinal reinforcement ratio). Next, the adequacy of the selected $\boldsymbol{x_{sl}}$ is verified based on the results of structural design for the static load combinations that requires solely knowledge of $\boldsymbol{x_{cd}}$. If the candidate design is acceptable, then the nonlinear structural analysis finite element model for the purposes of performance-based seismic design is composed. This model requires knowledge of M_y, θ_y and EI_{eff} of all structural members ends that can be directly calculated by the selected $\boldsymbol{x_{cd}}$ and $\boldsymbol{x_{sl}}$ design sub-vectors. Using the developed finite element model, chord rotation demands θ_{Ed} are calculated first for the OP and IU Limit States. These are compared with the corresponding limit values that are solely a function of the yield chord rotations θ_y, that are determined by $\boldsymbol{x_{cd}}$ and $\boldsymbol{x_{sl}}$ from Eq. (2). If the SLS constraints are satisfied, then the *EDP*s in terms of chord rotations and shear forces are calculated for the LS and CP Limit States. Based on these *EDP* values and the selected $\boldsymbol{x_{cd}}$ and $\boldsymbol{x_{sl}}$ sub-vectors, the transverse steel reinforcement sub-vector $\boldsymbol{x_{sw}}$ is chosen to provide adequate ${\theta^{pl}}_{u,k}$ and V_{Rd} capacities so that the performance checks of the ULS are satisfied. In addition,

the selected $\boldsymbol{x_{sw}}$ should satisfy the transverse reinforcement requirements and detailing rules for static loads and be consistent with construction practice. If the selection of $\boldsymbol{x_{sw}}$ to satisfy all corresponding constraints is successful, the candidate design is branded as feasible and its objective function value is returned to the optimizer. Otherwise, the solution is considered as not feasible and a penalty term is added to the value of the objective function.

The second strategy (Fig. 2b) is the one proposed in this study because it reduces greatly the search space of the optimization algorithm driving to more computationally efficient optimum solutions. According to this strategy, the optimizer selects only the cross-sectional dimensions design sub-vector $\boldsymbol{x_{cd}}$. Knowing $\boldsymbol{x_{cd}}$ and after checking for construction practice limitations, structural analysis for the static load combination is conducted and the required longitudinal steel reinforcement areas are calculated using standard structural design procedures. Then, an initial $\boldsymbol{x_{sl}}$ design sub-vector is selected that satisfies both longitudinal steel reinforcement area requirements and detailing rules for static loads in the most cost-efficient way. In fact, this task is an independent optimization problem that is typically resolved with negligible computational cost using exhaustive search or any other optimization algorithm. Having established $\boldsymbol{x_{cd}}$ and the initial $\boldsymbol{x_{sl}}$ sub-vectors, an initial nonlinear finite element model is composed and the corresponding θ_{Ed} demands are calculated for the OP and IU Limit States and compared to the respective limit values θ_{lim} (see Table 1) similarly to the standard solution strategy. In the proposed methodology, however, if the SLS performance constraints are not satisfied (i.e. $\theta_{Ed} > \theta_{lim}$) then an iterative procedure is launched, where the $\boldsymbol{x_{sl}}$ is successively modified until these constraints are satisfied.

More particularly, for each member end section and for both Serviceability Limit States (i.e. OP and IU), the required yield moment value M_y^{req} of the new iteration step is estimated by Eq. (6) from the yield moment M_y and ratio $\theta_{Ed} / \theta_{lim}$ calculated at the same section using the $\boldsymbol{x_{sl}}$ sub-vector of the previous step. Next, the required longitudinal steel reinforcement areas are calculated based on either the estimated M_y^{req} for both SLS or the static load combination, whichever is more demanding. Then, the design sub-vector $\boldsymbol{x_{sl}}$ of the new iteration step is selected to satisfy the required steel reinforcement areas as well as construction practice and static loads detailing rules in the most efficient manner. The afore-described procedure is repeated until the OP and IU Limit States constraints are satisfied.

$$M_{y,SLS}^{req} = M_{y,SLS} \cdot \left(\frac{\theta_{Ed}}{\theta_{lim}}\right)_{SLS} \quad (SLS = OP, IU) \tag{6}$$

Equation (6) is inspired by the "equal displacement rule" of Single Degree of Freedom Systems (SDOFs). According to this rule, an elastoplastic SDOF system develops the same maximum displacement response as that of an infinitely elastic system with the same mass, damping and elastic stiffness. It has been found (Panagiotakos and Fardis 1999, MC2010) that this rule applies well on average for local member deformations of concrete structures and especially the regular ones. This is the case because concrete structures have fundamental periods (estimated using EI_{eff}) that are in the range where the equal displacement rule applies fairly well for SDOF systems.

However, the proposed methodology does not rely on elastic analyses to calculate seismic demands and therefore is not limited by the approximations of the equal deformation rule. On the contrary, it uses rigorous nonlinear structural analysis procedures that calculate accurately local deformation demands. Therefore, performance checks are always reliably satisfied. This effectively means that the proposed approach can also be applied to concrete structures, where the equal deformation rule does not hold reliably (e.g. irregular structures).

Figure 3 demonstrates the equal deformation rule used herein in terms of member chord rotations. An elastoplastic response with the yield moment M_y of the previous iteration step,

an elastoplastic response with the required yield moment of the new step M_y^{req} and a fully elastic response are shown. All responses are controlled by the same EI_{eff} value and therefore are expected to develop the same chord rotation demand θ_{Ed}. The deformation limit value for the previous iteration step is $\theta_{lim} = \mu_{\theta,lim} \cdot \theta_y$, where $\mu_{\theta,lim}$ is the limit chord-rotation ductility with $\mu_{\theta,lim} = 1$ for the OP and $\mu_{\theta,lim} = 2$ for the IU Limit States respectively (see Table 1). As shown in Fig. 3, θ_{Ed} exceeds θ_{lim} and therefore the SLS performance constraint is not satisfied in the previous iteration step. For the performance constraint to be satisfied, the required deformation limit $\theta_{lim}^{req} = \mu_{\theta,lim} \cdot \theta_y^{req}$ of the new iteration step should be equal to the deformation demand θ_{Ed}. θ_y^{req} is the required yield chord-rotation corresponding to the required yield moment M_y^{req} of the new iteration step. From the geometry of Fig. 3, it holds that $\theta_{lim}^{req} = \mu_{\theta,lim} \cdot \theta_y^{req} = \mu_{\theta,lim} \cdot \theta_y \cdot (M_y^{req} / M_y) = \theta_{lim} \cdot (M_y^{req} / M_y)$. By setting $\theta_{lim}^{req} = \theta_{Ed}$ and solving for M_y^{req}, Eq. (6) is derived. It is worth noting here that the same procedure is used for both Serviceability Limit States and that Eq. (6) can be used also to reduce the required yielding moment of the new iteration step M_y^{req}, when the performance criteria are conservatively satisfied, leading to more cost-efficient solutions.

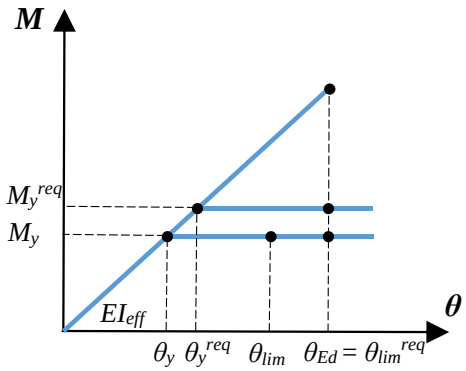

Fig. 3: Equal deformation rule

As discussed previously, Eq. (6) is based on the equal deformation rule at the member end sections level using the EI_{eff} values of the previous iteration step (Fig. 3). The latter is not accurate since EI_{eff} is directly proportional to the yield moments of reinforced concrete members end sections (see Eq. 5). Due to these approximations, an iterative procedure is required. It is noted, however, that application of the proposed iterative scheme to the case studies presented later in this study shows that convergence is rapid (typically 1-4 iterations are needed). This can be attributed to the proportional nature of the correction procedure (the more the chord rotation limit values are exceeded the more the M_y values are increased) and the fact that the provided steel reinforcement areas are often greater than the required due to the limitations in available steel bar diameters in construction practice. To further increase the convergence rate of the proposed procedure, M_y^{req} in Eq. (6) can be multiplied by a factor ξ greater than unity ($\xi \geq 1$). However, ξ should be kept as close as possible to unity since over-conservative designs may be derived otherwise.

After satisfying SLS constraints, the *EDP* values are calculated for the LS and CP Limit States and then an appropriate $\boldsymbol{x_{sw}}$ is chosen in a similar fashion to the standard solution strategy. If the selection of an appropriate $\boldsymbol{x_{sl}}$ sub-vector to meet SLS objectives and the selection of an appropriate $\boldsymbol{x_{sw}}$ sub-vector to fulfil the ULS objectives are successful, then the candidate designs are branded as feasible and the value of the objective function is calculated. Otherwise, the solution is treated as not feasible and a penalty term is added. The values of the objective functions are then returned to the optimizer to select the new $\boldsymbol{x_{cd}}$ sub-vectors.

From the previous discussion, the advantages of the proposed solution strategy become apparent. In the proposed approach, only the $\boldsymbol{x_{cd}}$ variables are treated as independent design

variables by the optimization algorithm, whereas the x_{sl} and x_{sw} sub-vectors are subsequently determined from x_{cd}. In the standard approach, both x_{cd} and x_{sl} sub-vectors are considered as independent design variables and only the x_{sw} sub-vector is later defined. Hence, the proposed approach drives to a great reduction of the required independent design variables considering that typical beam and column series of reinforced concrete frames are prismatic with different longitudinal steel reinforcement at the various end sections and in the case of beam members different top and bottom steel reinforcement.

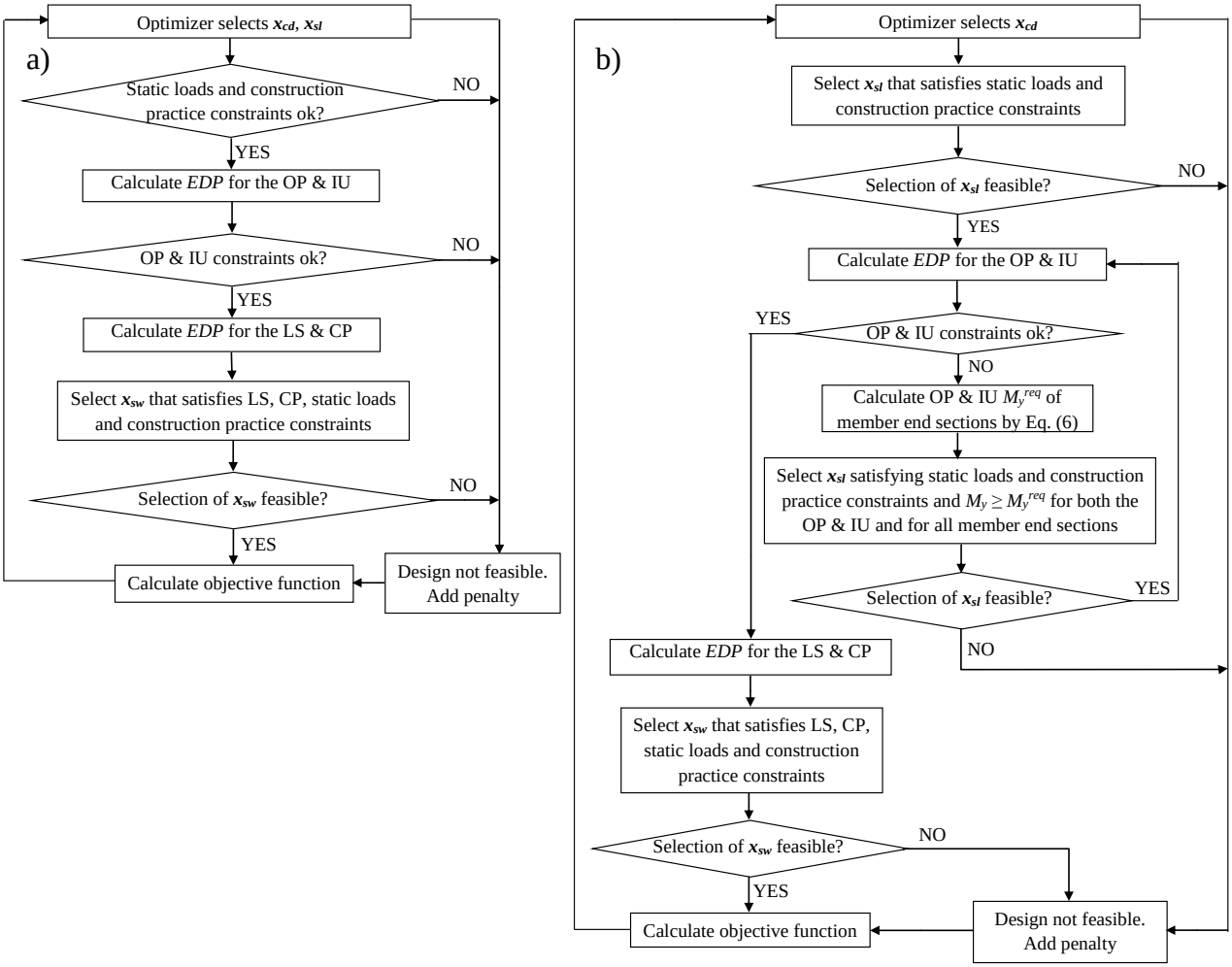

Fig. 2: Flowcharts of optimum seismic design strategies a) standard; b) proposed approach

2.6 Solution algorithms

For small scale discrete optimization problems, exhaustive search can be employed. For larger scale problems, metaheuristic optimization algorithms can be used instead (Yang 2014). In this study, the GA implemented in MATLAB-R2017a (Mathworks 2017) is applied. GAs (Holland 1975) are metaheuristic optimization algorithms imitating Darwin's theory of evolution. They gradually modify populations (generations) of candidate design vectors $\boldsymbol{x}$ (individuals). Individuals of next generations (children) are formed from selected individuals of previous generations (parents) based on their objective function values. The algorithm adopted herein is capable of handling discrete design variables by using special crossover and mutation functions (Deep *et al*. 2009). It is emphasised, however, that the solution procedures proposed

in this study can be applied by employing any other automated optimization algorithm that treats discrete design variables.

3 Optimum seismic design of RC frames applications

3.1 Introduction

In this section, applications of the optimum seismic design methodologies described previously to reinforced concrete frames are presented. The goal is to compare the computational performance of the different solution strategies and investigate the applicability of the proposed approach. More particularly, a simple portal, a 3-storey 3-bay and a 6-storey 2-bay reinforced concrete frames are designed in accordance with the deformation and performance-based methodology of MC2010. Since no specifications are provided in MC2010 for the serviceability checks of non-structural components, these checks are conducted herein by limiting inter-storey drifts according to EC8-Part 1 (CEN 2004) recommendations for buildings with brittle non-structural elements. Nonlinear structural analyses are conducted with the general finite element program for the inelastic damage analysis of structures IDARC2D Version 7.0 (Reinhorn *et al*. 2007) developed at the State University of New York at Buffalo. The analyses are performed on a personal computer using each time one core of an Intel i5-7500 processor with operating frequency 3.40 GHz.

3.2 Portal frame

In this section, a simple portal reinforced concrete frame (Fig. 4) is optimally designed. The span of the frame is 4m and the height 3m. Concrete C25/30 and reinforcing steel B500C in accordance with EC2 specifications are used. Concrete cover is assumed to be 30mm. Storey weight for the quasi-permanent combination is 288kN and it is applied in the form of two equal vertical point loads at the locations of the columns. The reinforced concrete frame is part of a building of ordinary importance that rests on soil class B according to the classification of EC8 – Part 1. It is designed for 0.36g peak ground acceleration (PGA) for the 10/50 seismic hazard level. PGAs for the other seismic hazard levels of MC2010 (Table 1) are calculated by multiplying the 10/50 values by the importance factor γ_I calculated by the equation proposed in EC8. Pushover analysis is employed to calculate seismic demands of this frame in accordance with the N2 method as prescribed in EC8.

Due to symmetry, columns C1 and C2 are assumed to have the same section and the beam the same end sections and the same top and bottom longitudinal reinforcement. Moreover, for simplicity, square sections are used for the column members. Furthermore, it is assumed that the longitudinal and transverse reinforcement do not vary along members' length. In this manner, only one cross-section is required for the column members and one cross-section for the beam member.

It is considered that the column cross-sectional dimensions and the beam height can take discrete values starting from 0.25 m and increasing by 0.05 m up to 0.80 m. Beam width is assumed to be 0.25 m. Longitudinal bar diameters of 14 mm and transverse bar diameters of 8mm are used for the beam and column members. Transverse reinforcement spacing may take values starting from 0.10 m and increasing by 0.025 m up to 0.30 m. The number of longitudinal steel bars and legs of the transverse reinforcement can take any integer value between 2 and 6 for all frame members.

Following the previous design assumptions, 4 independent design variables are required for the standard solution strategy. These are the square column cross-sectional dimension, the

beam height, the number of longitudinal steel bars per side of the column sections and the number of the top or bottom steel reinforcing bars of the beam member. The possible combinations of these 4 design variables are 3600. On the other hand, for the proposed solution strategy, 2 independent design variables are required (columns cross-sectional dimension and beam height) with only 144 possible combinations.

Due to the rather small scale of this problem, exhaustive search is used to derive the optimum solutions. The main advantage of this method is that it is guaranteed to provide the global optimum solution. Using the standard solution strategy, the analysis was terminated after 3170 secs and the optimum cost was found to be 511.1 € corresponding to the solution provided in Table 2. Using the proposed strategy, the exhaustive search was terminated after 125 secs (approximately 25 times faster) yielding the same solution as the standard approach. This observation shows both the computational efficiency and validity of the proposed approach. It should be clarified here that the computational times reported have only relative value since they generally depend on many issues not directly related to the proposed methodology (e.g. speed of reading the output files of the finite element analysis program from MATLAB). However, in this study, the standard and the proposed methodologies use similar procedures and therefore their computational times can be directly compared.

It is interesting to discuss at this point the convergence of iterations used in the proposed methodology to select the appropriate $\boldsymbol{x_{sl}}$ sub-vector following the selection of the optimal sub-vector $\boldsymbol{x_{cd}}$ by the optimizer shown in Table 2. The initial (1st iteration) $\boldsymbol{x_{sl}}$ sub-vector selected to satisfy static loads and construction practice constraints fails to satisfy OP and IU Limit States constraints. If SoV is defined as the sum of constraints violations $g_j(x)$, given by Eq. (4) when positive and taken as zero when negative, for all end sections and for both Limit States then SoV is found approximately equal to 1.9 for the 1st iteration. Hence, a second $\boldsymbol{x_{sl}}$ sub-vector is selected, based on the procedure shown in Fig. 2b, for which SoV drops rapidly to approximately 0.1. In the 3rd iteration, SoV is zero and the selection of the $\boldsymbol{x_{sl}}$ sub-vector (presented in Table 2) becomes feasible.

Figure 5 presents MC2010 checks of rotation and shear force constraints (Eq. 4) for all Limit States as obtained for the optimum solution of Table 2. Column sections are defined by the column member number (e.g. C01) and a letter designating the location of the section in the member (i.e. B=bottom and T=top). Similarly, beam sections are defined by the beam member number (e.g. B01) and a letter designating the location of the section in the member (i.e. L=left and R=right). Limit States are stated by the acronyms shown in Table 1. It is evident that all constraints checks are satisfied and the optimum solution is feasible.

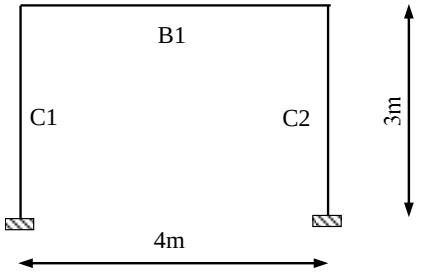

Fig. 4: Reinforced concrete portal frame

Table 2: Portal frame optimum design solution obtained by the standard and proposed approach

Members	**Columns**							**Beams**								
Property	h_c	b_c	n_c	d_{bc}	n_{wc}	d_{bwc}	s_c	h_b	b_b	n_{tb}	d_{bt}	n_{bb}	d_{bb}	n_{wb}	d_{bwb}	s_b
Units	m	m		mm		mm	m	m	m		mm		mm		mm	m
	0.40	0.40	4	14	2	8	0.15	0.40	0.25	4	14	4	14	2	8	0.25

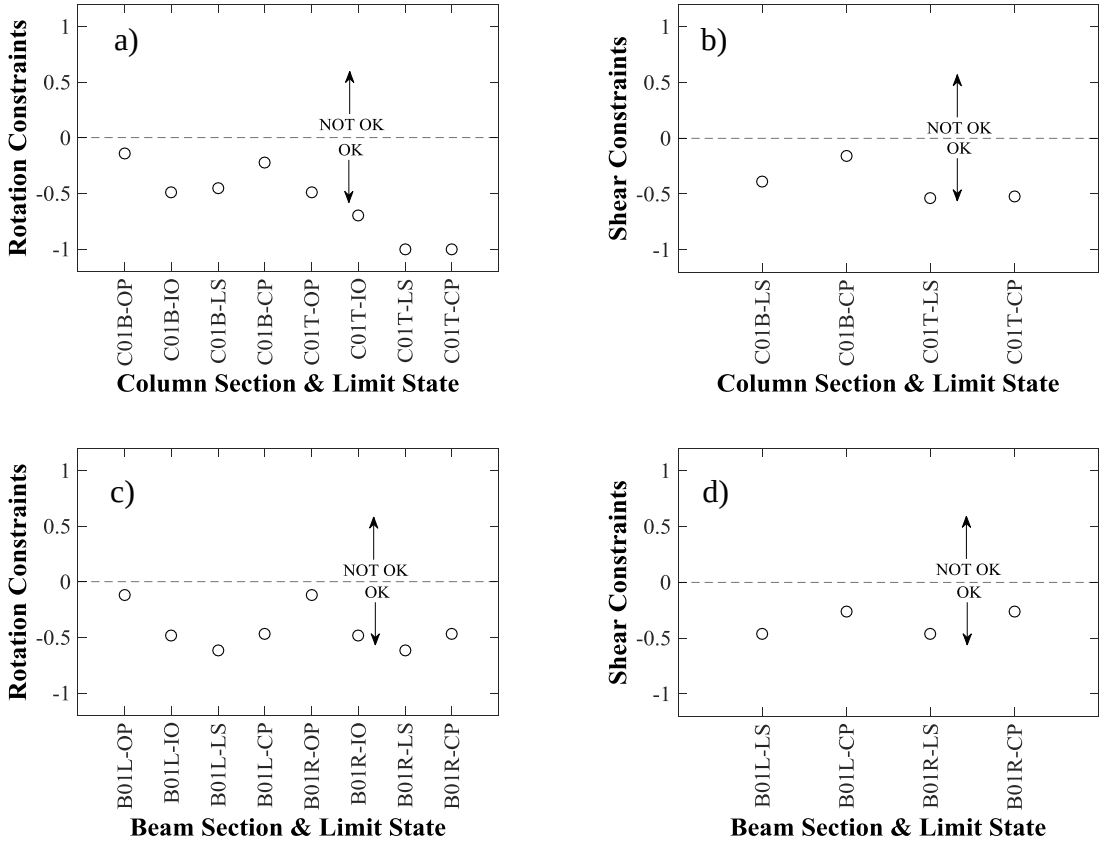

Fig. 5: MC2010 chord rotation and shear force constraints checks of the reinforced concrete portal frame optimum design solution obtained by the standard and proposed solution strategy

3.3 Three-storey three-bay frame

In this section, a three-storey three-bay reinforced concrete frame (Fig. 6) is examined. Frame spans are 5 m and storey heights 3 m. Concrete C25/30 and reinforcing steel B500C are used. Concrete cover is assumed to be 30mm. Storey weight for the quasi-permanent combination is 864 kN and it is applied in the form of vertical point loads of 144 kN at the locations of the exterior and 288 kN at the interior columns. The frame is part of a building of ordinary importance that rests on soil class B. It is designed for 0.36g peak ground acceleration (PGA) for the 10/50 seismic hazard level. Pushover analysis is employed to calculate seismic demands of this frame following the N2 method. For simplicity, an invariant lateral load pattern proportional to lateral forces consistent with the 1st mode of vibration is used in the pushover analysis of this low-rise and regular in elevation frame.

For simplicity, square sections are assumed for the column members that are different for the exterior and interior columns. Furthermore, column cross-sectional dimensions do not change along frame height. The steel reinforcement is assumed uniform along the length of column members, but may change between different storeys. Beam cross-sectional heights do not change inside storeys but can be different for the different storeys. The same beam width is assumed for all storeys of the frame that cannot be greater than the column sections. Different steel reinforcement is used for the exterior and interior supports of the beam series. The same top and bottom steel reinforcement is applied for the beam sections due to symmetry. It is interesting to note that this observation must be applied externally by the user in the case of the standard solution strategy reducing significantly its independent design variables. In the case of the proposed methodology, however, this feature is derived automatically by the

solution procedure and has no effect on the number of the independent design variables. This shows the versatility of the proposed approach.

In addition to the previous, it is assumed herein that column cross-sectional dimensions and beam heights take values starting from 0.30 m and increasing by 0.05 m up to 1.00 m. Beams width is assumed to take one of the following values: 0.30 m, 0.35 m and 0.40 m. Longitudinal bar diameters of 16 mm and transverse bar diameters of 8 mm are used for all concrete members. Transverse reinforcement spacing takes values starting from 0.10 m and increasing by 0.025 m up to 0.30 m. The number of longitudinal steel bars and legs of the transverse reinforcement can take any integer value between 2 and 10 for all frame members.

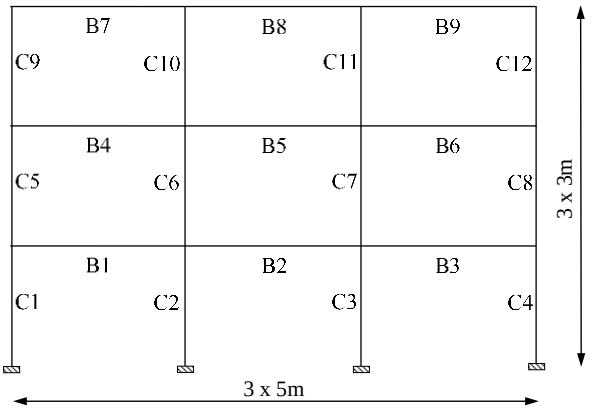

Fig. 6: Reinforced concrete three-storey three-bay frame

Following the previous assumptions and due to symmetry, 6 different column sections and 6 beams sections are applied. The locations of these sections are shown in Tables 3 and 4. Furthermore, 6 independent design variables are required by the proposed approach (2 column cross-sectional dimensions, 3 beam heights and 1 beam width) and 18 design variables by the standard strategy (6 cross-sectional dimensions plus the numbers of longitudinal bars of the 6 beam and 6 column sections).

Due to the larger scale of this problem, the GA described in §2.6 is employed for its solution. For both solution strategies, a population size of 100 individuals with 5 elite individuals as recommended in Mathworks (2017) for an optimization problem with 18 design variables as the case of the standard approach. A smaller population size is recommended in MATLAB for the 6 design variables of the proposed approach. However, it was decided to use the same population size for both methodologies so that this parameter will not affect their comparison.

It is important to clarify at this point that more than one iterations may be required by the proposed strategy for each candidate design. Therefore, a comparison of the number of individuals and generations examined by the two solution approaches is not directly reflecting their computational costs (it would favour the proposed approach). Hence, it was decided to compare the two methodologies in terms of their performance with respect to computational time. To serve this goal, all GA analyses were terminated 8 hours after start and their obtained minimum objective function values were compared. To account for the stochastic nature of GA analyses, 10 independent GA runs were performed for each solution strategy.

Fig. 7a compares the minimum costs of all GA analyses obtained for both solution strategies. It is evident that the proposed methodology leads to an optimum solution that is 6% (4244 € instead of 4502 €) less expensive than the standard methodology. The structural configuration of the optimum solution from the proposed approach is shown in Tables 3 and 4. Furthermore, to examine the variability of the GA predictions, Fig. 7b presents the minimum

costs obtained from all GA runs for both solution methodologies in the form of box plots. The box plots show the minimum, maximum and median (red line) minimum costs obtained from the 10 GA runs. Inside the boxes, the 25^{th} to 75^{th} percentile solutions are contained. The mean minimum cost prediction of the proposed approach is 8% less expensive than the standard solution. It is noteworthy that the best prediction of the standard approach is worse than the worst prediction of the proposed methodology. It is also significant to observe that the variability of the proposed method is significantly lesser than the standard approach (i.e. Coefficient of Variation 1.7% instead of 7.2%).

Moreover, Fig. 7c shows the variation of minimum costs with time of the optimum cost solutions presented in Fig. 7a. It can be concluded that the solution based on the proposed strategy is always more cost efficient than the standard approach. Fig. 7d presents the variation of the same costs with the number of generations produced by the GA optimizer in the time span of 8 hours. The GA produces almost 10 times more generations and individuals in the standard approach with respect to the proposed methodology. This does not mean, however, that the candidate designs of the proposed methodology require on average 10 iterations to converge to the selection of the longitudinal reinforcement so that both approaches conduct the same number of nonlinear analyses. Most of the individuals of the standard methodology fail to satisfy the early detailing constraints set by EC2 (e.g. maximum and minimum longitudinal reinforcement ratio, distance between longitudinal bars) for the design against static loads since the $\boldsymbol{x_{cd}}$ and $\boldsymbol{x_{sl}}$ sub-vectors are chosen arbitrarily by the optimizer. These individuals are computationally inexpensive as they are not subjected to nonlinear analyses to avoid unnecessary computational cost (Fig. 2a). Furthermore, the standard approach designs that fail to satisfy the OP and IU constraints are not subjected to nonlinear analyses for the LS and CP Limit States (Fig. 2a). In the proposed approach, however, all candidate designs are subjected to nonlinear analyses for all Limit States. At this point, it is important to recall that a smaller population size is recommended in MATLAB for the 6 design variables of the proposed approach (60 instead of 100). This would lead to more generations for the proposed approach and even better performance in the same time span.

Figure 7e presents the progress of SoV, as defined in §3.2, with the number of iterations for the optimum design solution presented in Tables 3 and 4. SoV drops rapidly and monotonically from approximately 3.8 for the 1^{st} iteration to 0 for the 5^{th} iteration, where the selection of $\boldsymbol{x_{sl}}$ sub-vector is branded as feasible. In these analyses, it is assumed that $\xi = 1$. To investigate the influence of ξ on the convergence of the $\boldsymbol{x_{sl}}$ selection, the design of $\boldsymbol{x_{sl}}$ for the same $\boldsymbol{x_{cd}}$ sub-vector of Tables 3 and 4 is repeated with $\xi = 1.1$. As shown in Fig. 7e, the convergence of SoV to zero is significantly faster with only 3 iterations required to select an appropriate $\boldsymbol{x_{sl}}$ sub-vector. However, this improvement of computational performance comes with an increase in the optimum cost of the reinforced concrete frame from 4244 € to 4306 € (1%).

Moreover, Fig. 7f shows the variation with time of the mean values of the minimum costs of the 10 GA runs using the standard and the proposed approach. Again, the proposed approach exhibits better performance along the entire time span of the GA runs. The cost savings are even more important at the first stages of the GA runs. It is also important to note that the means of the predictions of the proposed approach tend to stabilize after 7 hours meaning that this methodology, on average, reaches convergence. This is not the case for the standard approach.

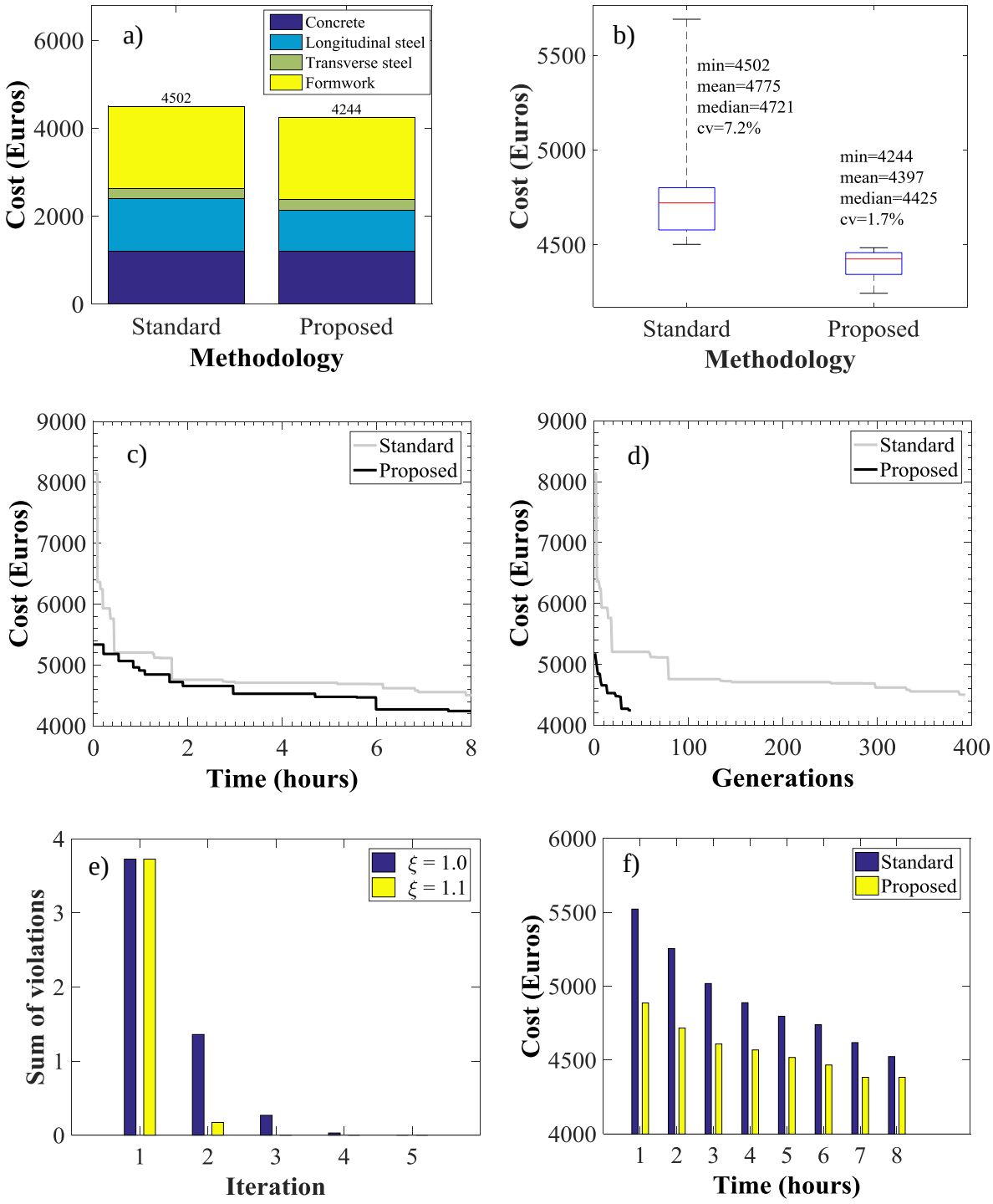

Fig. 7: Comparison of the computational performance of the standard and proposed solution strategies for the 3-storey 3-bay reinforced concrete frame

Figure 8 shows the checks of rotation and shear force constraints according to MC2010 for all Limit States as obtained for the two optimum solutions of Fig. 7a. For clarity, only the checks that contain one constraint value greater than -0.25, either for the standard or the proposed solution strategy, are presented. It is evident that all constraints checks are satisfied and the optimum solutions are feasible. It is interesting to observe that in many cases the constraints are very close to the limit zero value, which shows the efficiency of the derived optimum solutions.

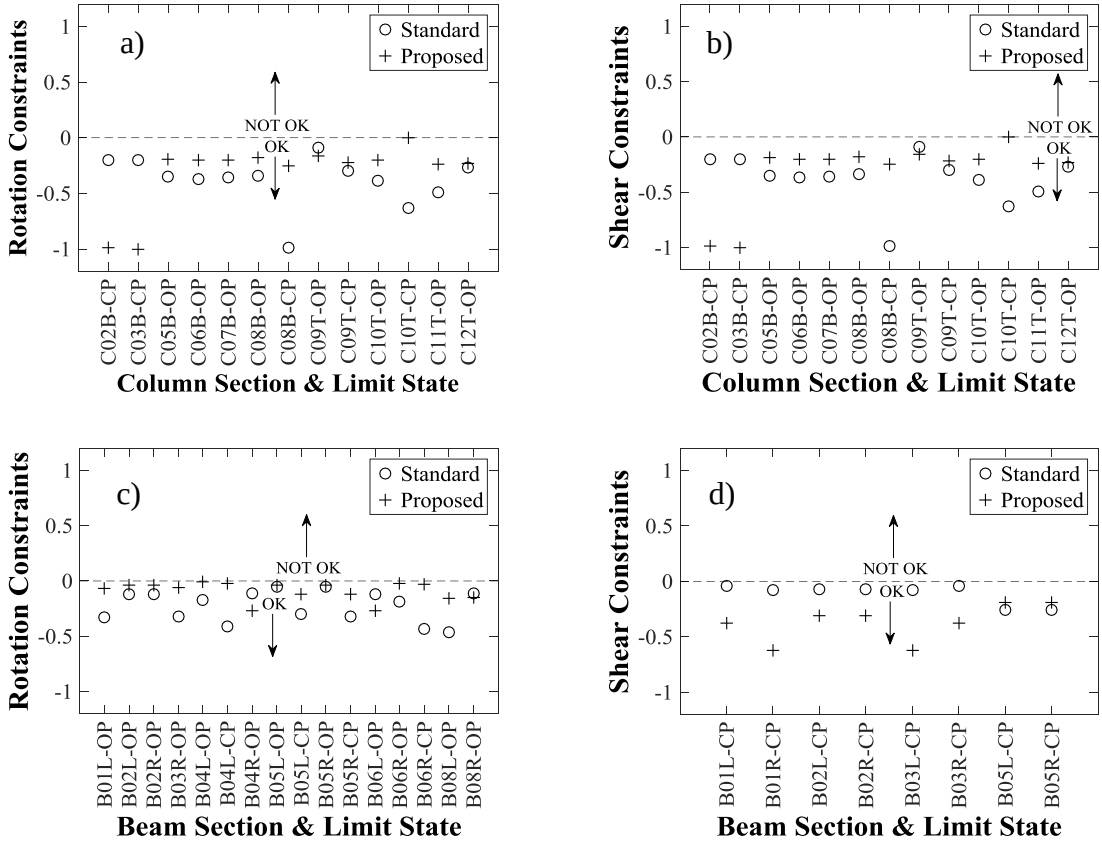

Fig. 8: MC2010 chord rotation and shear force constraints checks of the best reinforced concrete 3-storey 3-bay frame design solutions obtained by the standard and proposed solution strategy

Table 3: Columns detailing of the 3-storey 3-bay frame optimum design solution obtained by the proposed approach

	Property:	h_c	b_c	n_c	d_{bc}	n_{wc}	d_{bwc}	s_c
Sections	**Locations**	m	m		mm		mm	m
1	C1, C4	0.3	0.3	3	16	2	8	0.175
2	C2, C3	0.5	0.5	4	16	2	8	0.175
3	C5, C8	0.3	0.3	2	16	2	8	0.175
4	C6, C7	0.5	0.5	3	16	3	8	0.1
5	C9, C12	0.3	0.3	2	16	2	8	0.175
6	C10, C11	0.5	0.5	2	16	2	8	0.125

Table 4: Columns detailing of the 3-storey 3-bay frame optimum design solution obtained by the proposed approach

	Property:	h_b	b_b	n_{tb}	d_{bt}	n_{bb}	d_{bb}	n_{wb}	d_{bwb}	s_b
Sections	**Locations**	m	m		mm		mm		mm	m
1	B1L, B3R	0.65	0.3	2	16	2	16	2	8	0.3
2	B1R, B2L, B2R, B3L	0.65	0.3	4	16	4	16	2	8	0.3
3	B4L, B6R	0.3	0.3	4	16	4	16	2	8	0.175
4	B4R, B5L, B5R, B6L	0.3	0.3	6	16	6	16	2	8	0.175
5	B7L, B9R	0.4	0.3	2	16	2	16	2	8	0.25
6	B7R, B8L, B8R, B9L	0.4	0.3	2	16	2	16	2	8	0.25

3.4 Six-storey two-bay frame

In this section, a six-storey two-bay reinforced concrete frame (Fig. 9) is optimally designed. Frame spans are 5 m and storey heights 3 m. Concrete C25/30 and reinforcing steel B500C are used. Concrete cover is assumed to be 30mm. Storey weight for the quasi-permanent combination is 576kN and it is applied in the form of vertical point loads of 144kN at the exterior and 288kN at the interior joints. The frame is part of a building of ordinary importance that rests on soil class B. It is designed for 0.24g peak ground acceleration (PGA) for the 10/50 seismic hazard level. Based on this information, the EC8 – Part 1 elastic pseudo-acceleration response spectrum for regions of high seismicity is composed, as shown in Fig. 10b, that serves as the target response spectrum in this study.

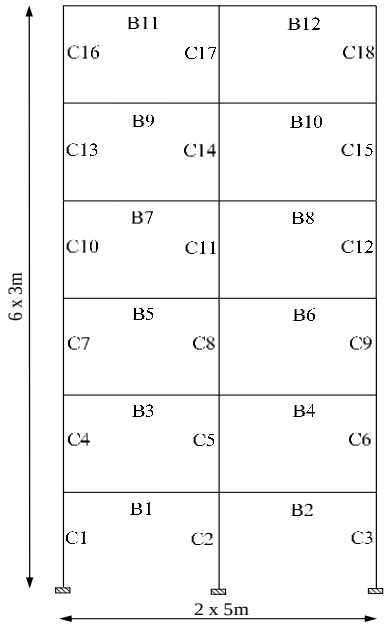

Fig. 9: Reinforced concrete six-storey two-bay frame

The frame is designed to resist the Tabas 1978 earthquake ground motion as recorded at station ST59 in the X-direction and scaled in amplitude (Fig 10a) so that its elastic response spectrum is not lower than 90% of the target response spectrum as shown in Figure 10b and in accordance with the recommendations of MC2010. Nonlinear response-history analysis is employed to calculate seismic demands of this frame to demonstrate the applicability of the proposed methodology when using also this nonlinear structural analysis procedure. It is clarified that according to MC2010, at least 3 ground motions are required to use maximum and 7 ground motions to use average response values in the seismic design of concrete structures. However, the main objective of this section is to compare the performance of the different solution strategies. Therefore, it was deemed more appropriate to focus on a single ground motion record rather than repeating a great number of nonlinear response history analyses.

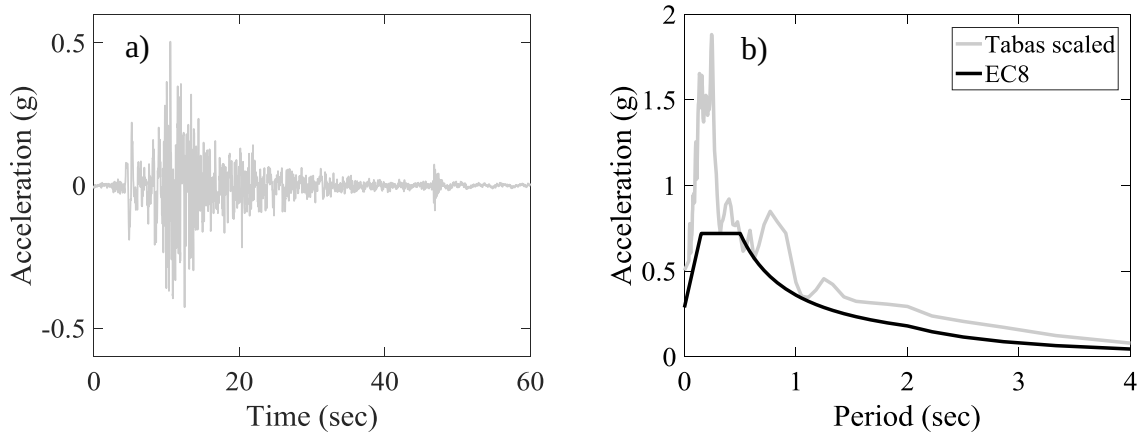

Fig. 10: Tabas 1978 scaled ground motion: a) acceleration time history; b) elastic response spectrum

The same simplifications and assumptions are made for the detailing of the 6-storey 2-bay frame of this section as in §3.3. The only difference in this frame is that it is assumed, for simplicity reasons, that the cross-sectional dimensions of the beam members and the steel reinforcement of both the beam and column members are changed every 2 storeys rather than each storey. Following these assumptions and due to symmetry, 6 different column sections and 6 beams sections are required. The locations of these sections are shown in Tables 5 and 6. In total, 6 independent design variables are required by the proposed approach (2 column cross-sectional dimensions, 3 beam heights and 1 beam width) and 18 design variables by the standard strategy (cross-sectional dimensions plus the numbers of longitudinal bars of the 6 beam and 6 column sections). Furthermore, the cross-sectional dimensions and steel reinforcement variables are assumed to take values from the same discrete variables sets as in §3.3. Again, the GA described in §2.6 is applied herein for both solution strategies with a population size of 100 individuals and 5 elite individuals. Ten independent GA runs were conducted for each solution methodology that lasted 8 hours each.

Fig. 11a compares the minimum costs of all GA analyses obtained for both solution strategies. The proposed strategy yields an optimum solution with 21% (5391 € instead of 6820 €) less cost than the standard approach. The structural configuration of the optimum solution from the proposed methodology can be found in Tables 5 and 6. In addition, Fig. 11b illustrates the minimum costs obtained from all GA runs for both solution methodologies in the form of box plots as in §3.3. It is shown that the mean minimum cost prediction of the proposed approach is 28% less expensive than the standard solution. It is noted that the best prediction of the standard approach is significantly worse than the worst prediction of the proposed methodology. Moreover, the variability of the proposed method is smaller than the standard approach (i.e. Coefficient of Variation 3.5% instead of 6.0%).

Furthermore, Fig. 11c presents the variation of minimum costs with time of the optimum cost solutions presented in Fig. 11a. It is evident that the proposed solution is continuously less costly than the standard approach. Additionally, Fig. 11d shows the variation of the same costs with the number of generations produced by the GA for both design approaches and in the same time length. Very similar comments to the respective figure of §3.3 can generally be made. Moreover, Fig. 11e presents the variation with time of the mean values of the minimum costs of the 10 GA runs using the standard and the proposed methodologies. Again, the proposed methodology exhibits significantly better performance along the entire time span of the GA solutions. It is also noted that the means of the predictions of the proposed approach tend to converge, which is not the case for the standard methodology.

Regarding the convergence in the selection of x_{sl} for the optimal x_{cd} sub-vector of Tables 5 and 6, it is immediate in this case because the x_{sl} sub-vector selected to fulfil the static loads constraints is also found to satisfy the OP and IU Limit States constraints.

Lastly, Fig. 12 presents rotation and shear force constraints checks of MC2010 for the two optimum solutions of Fig. 11a. Only the checks that contain one constraint value greater than -0.25, either for the standard or the proposed solution strategy are shown for illustration reasons. As expected, all constraints checks are satisfied and the optimum solutions are acceptable.

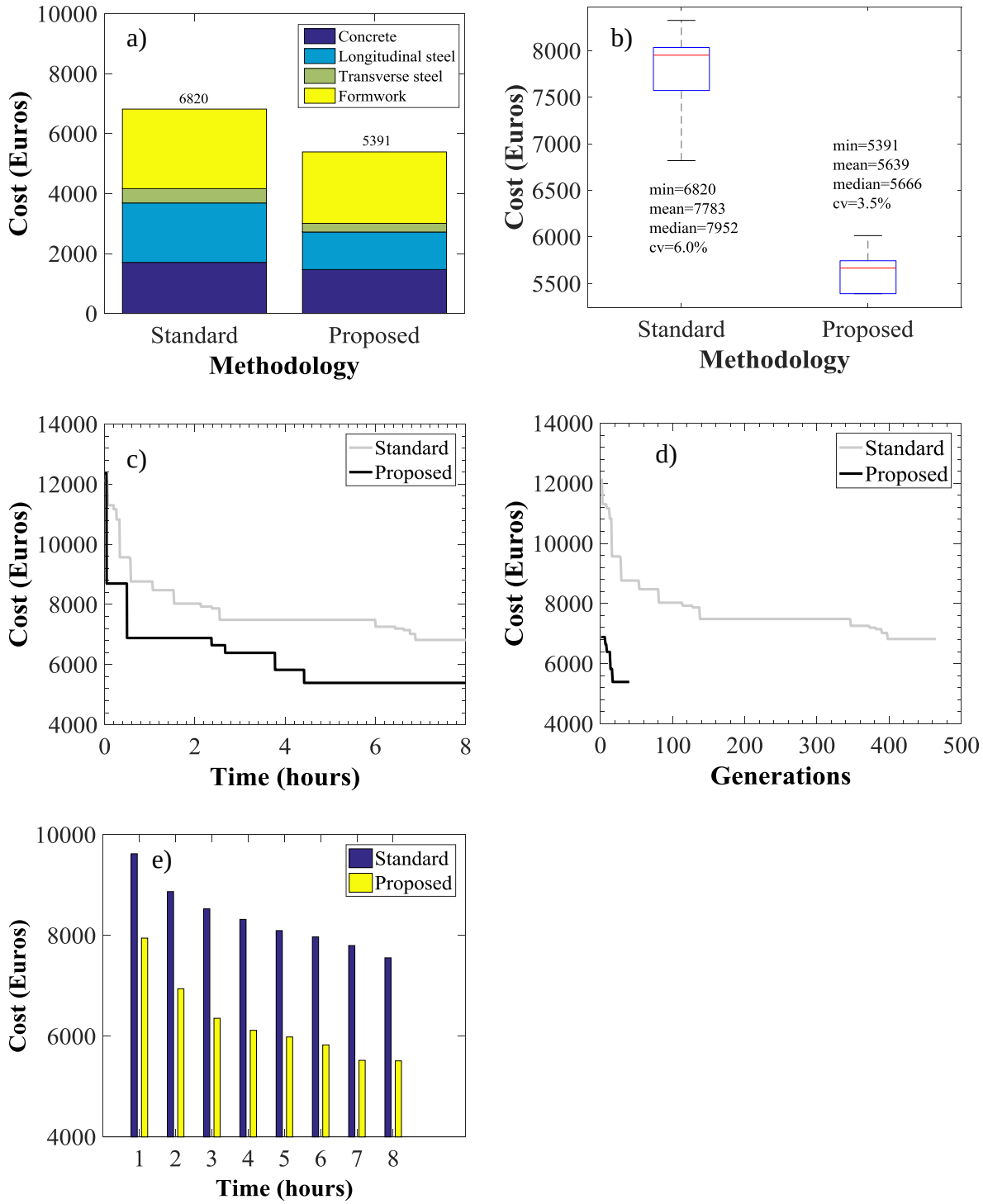

Fig. 11: Comparison of the computational performance of the standard and proposed solution strategies for the 6-storey 2-bay reinforced concrete frame

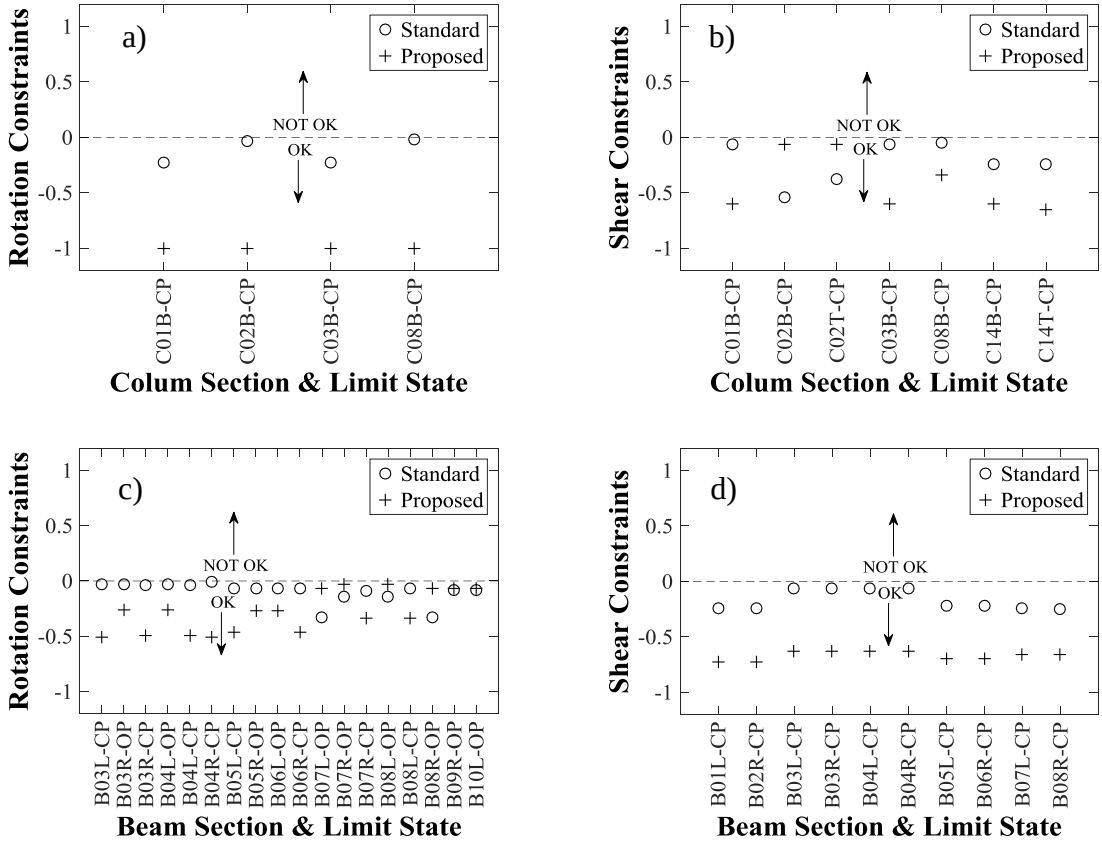

Fig. 12: MC2010 chord rotation and shear force constraints checks of the best reinforced concrete 6-storey 2-bay frame design solutions obtained by the standard and proposed solution strategy

Table 5: Columns detailing of the 6-storey 2-bay frame optimum design solution obtained by the proposed approach

	Property:	h_c	b_c	n_c	d_{bc}	n_{wc}	d_{bwc}	s_c
Sections	**Locations**	m	m		mm		mm	m
1	C1, C3, C4, C6	0.3	0.3	4	16	2	8	0.175
2	C2, C5	0.55	0.55	6	16	2	8	0.15
3	C7, C9, C10, C12	0.3	0.3	3	16	2	8	0.175
4	C8, C11	0.55	0.55	5	16	2	8	0.175
5	C13, C15, C16, C18	0.3	0.3	2	16	2	8	0.175
6	C14, C17	0.55	0.55	3	16	3	8	0.175

Table 6: Columns detailing of the 6-storey 2-bay frame optimum design solution obtained by the proposed approach

	Property:	h_b	b_b	n_{tb}	d_{bt}	n_{bb}	d_{bb}	n_{wb}	d_{bwb}	s_b
Sections	**Locations**	m	m		mm		mm		mm	m
1	B1L, B2R, B3L, B4R	0.4	0.3	2	16	2	16	2	8	0.25
2	B1R, B2L, B3R, B4L	0.4	0.3	2	16	2	16	2	8	0.25
3	B5L, B6R, B7L, B8R	0.3	0.3	2	16	2	16	2	8	0.175
4	B5R, B6L, B7R, B8L	0.3	0.3	2	16	2	16	2	8	0.175
5	B9L, B10R, B11L, B12R	0.3	0.3	2	16	2	16	2	8	0.175
6	B9R, B10L, B11R, B12L	0.3	0.3	2	16	2	16	2	8	0.175

4 Conclusions

Deformation- and performance-based seismic design offers direct control of structural damage for different levels of seismic hazard limiting losses caused by earthquakes. However, the number of applications and research studies on optimum performance- and deformation-based seismic design of reinforced concrete frames is rather limited. This observation can be mainly attributed to the computational cost of the nonlinear structural analysis procedures required to calculate reliably inelastic seismic demands and the great number of design variables required to describe the nonlinear response of these structural systems.

The present study develops a new computationally efficient strategy for the automated optimum deformation- and performance-based seismic design of reinforced concrete frames using nonlinear static and/or dynamic analysis procedures. The proposed methodology is based on a simple, deformation-based, iterative procedure that designs the steel reinforcement of concrete frames to meet their performance objectives provided the cross-sectional dimensions of their structural members. The longitudinal steel reinforcement is first selected to satisfy the Serviceability Limit States and the transverse steel reinforcement is then appropriately chosen to fulfil the Ultimate Limit States.

Following the proposed approach, only the cross-sectional dimensions of reinforced concrete frames should be set as independent design variables in the optimization problem. This drastically reduces the search space allowing the optimization algorithms to yield more cost efficient and robust optimum solutions.

The proposed solution strategy is applied to the design of various reinforced concrete frames according the *fib* Model Code 2010 deformation- and performance-based seismic design methodology. More particularly, a portal frame, a 3-storey 3-bay and a 6-storey 2-bay frames are examined. Additionally, the performance of the new methodology is compared with a more standard solution approach, where both the cross-sectional dimensions and the longitudinal steel reinforcement are used as independent design variables.

In the case of the simple portal frame, where exhaustive search is applied, it is found that the proposed approach yields the same global optimum as the standard approach in significantly less computational time. In the case of the other two frames, where a stochastic GA was employed, it is found that, in the same computational time, the proposed approach provides less costly and more robust design solutions than the standard methodology. Therefore, it is believed that the proposed solution strategy can become a valuable tool in the automated, optimum deformation- and performance-based seismic design of reinforced concrete frames with nonlinear structural analysis procedures. Nevertheless, further research is required to extend and validate the proposed methodology to complex, three dimensional reinforced concrete frames with a great number of design variables. Furthermore, additional considerations are needed to extend the developed methodology to address other types of concrete structures such as infilled frames, wall and dual systems.

References

ACI (2008) Building Code Requirements for Structural Concrete (ACI 318 – 08) and Commentary. American Concrete Institute, Farmington Hills, Michigan, USA

CEN (2000) Eurocode 2: Design of concrete structures. Part 1-1: General rules and rules for buildings. European Standard EN 1992-1-1, Brussels, Belgium

CEN (2004). Eurocode 8: Design of structures for earthquake resistance. Part 1: General rules, seismic actions and rules for buildings. European Standard EN 1998-1, Brussels, Belgium

Chan CM, Zou XK (2004) Elastic and inelastic drift performance optimization for reinforced concrete buildings under earthquake loads. Earthquake Eng Struct Dyn 33:929–950

Deep K, Singh KP, Kansal ML, Mohan C (2009) A real coded genetic algorithm for solving integer and mixed integer optimization problems. Appl Math Comput 212:505–518

Fardis (2009) MN. Seismic design, assessment and retrofitting of concrete buildings. Springer, Dordrecht, The Netherlands
Fardis MN (2013) Performance- and displacemenent-based seismic design and assessment of concrete structures in *fib* Model Code 2010. Struct Concrete 14:215-229
FEMA (1997) NEHRP guidelines for the seismic rehabilitation of buildings. Federal Emergency Management Agency, Washington, USA
fib (2003) Displacement-based seismic design of reinforced concrete buildings. Federation Internationale du Beton, Lausanne, Switzerland
fib (2012) Model Code 2010. Bulletins Nos. 65/66, Federation Internationale du Beton, Lausanne, Switzerland
Filippou FC, Ambrisi A, Issa A (1992) Nonlinear static and dynamic analysis of RC sub-assemblages. Report UCB/EERC-92/08, University of California, Berkeley, USA
Fragiadakis M, Papadrakakis M (2008) Performance-based optimum seismic design of reinforced concrete structures. Earthquake Eng Struct Dyn 37:825-844
Fragiadakis M, Lagaros ND (2011) An overview to structural seismic design optimization frameworks. *Comput Struct* 89:1155-1165
Ganzerli S, Pantelides CP, Reaveley LD (2000) Performance-based design using structural optimization. Earthquake Eng Struct Dyn 29:1677-1690
Gencturk B (2013) Life-cycle cost assessment of RC and ECC frames using structural optimization. Earthquake Eng Struct Dyn 42:61-79
Giberson MF (1967) The response of nonlinear multi-story structures subjected to earthquake excitation. PhD Thesis, California Institute of Technology, Pasadena, CA, USA
Holland J (1975) Adaptation in natural and artificial systems. University of Michigan Press, Ann Arbor, MI, USA
Kappos AJ, Stefanidou S (2010) A deformation-based seismic design method for 3D RC irregular buildings using inelastic dynamic analysis. Bull Earthquake Eng 8:875-895
Krawinkler H (1996) Pushover analysis: why, how, when, and when not to use it. Maui: Proceedings 1996 SEAOC Convention.
Lagaros ND, Fragiadakis M (2011) Evaluation of ASCE-41, ATC-40 and N2 static pushover methods based on optimally designed buildings. Soil Dyn Earthquake Eng 31: 77-90
Lagaros ND (2014) A general purpose real-world structural design optimization computing platform. J Struct Multidisciplinary Optim 49:1047-1066
MathWorks (2017). MATLAB R2017a – Global Optimization Toolbox. The MathWorks Inc, Natick, MA, USA
Mergos PE, Kappos AJ (2012) A gradual spread inelasticity model for R/C beam-columns accounting for flexure, shear and anchorage-slip. Eng Struct 44: 94-106
Mergos PE (2017) Optimum seismic design of reinforced concrete frames according to Eurocode 8 and *fib* Model Code 2010. Earthquake Eng Struct Dyn 46: 1181–1201
Mergos PE (2018) Seismic design of reinforced concrete frames for minimum embodied CO_2 emissions. Energ Buildings, https://doi.org/10.1016/j.enbuild.2017.12.039
Panagiotakos TB, Fardis MN (1999) Estimation of inelastic deformation demands in multistorey RC frame buildings. Earthquake Eng Struct Dyn 28:501-528
Panagiotakos TB, Fardis MN (2001) A displacement-based seismic design procedure of RC buildings and comparison with EC8. Earthquake Eng Struct Dyn 30:1439-1462
Priestley MJN, Calvi GM, Kowalsky MJ (2007) Direct displacement based seismic design of structures. IUSS Press, Pavia, Italy
Reinhorn A, Roh H, Sivaselvan M, Kunnath SK, Valles RE, Madan A, Li C, Lobo R, Park YJ (2007) IDARC2D Version 7.0: A program for the inelastic damage analysis of structures. MCEER-09-006 Report, State University of New York at Buffalo, Buffalo, USA
SEAOC (1995) Vision 2000, Performance based seismic engineering of buildings. USA: Structural Engineers Association of California, Sacramento, USA
Sivaselvan MV, Reinhorn A (2000) Hysteretic models for deteriorating inelastic structures. J Eng Mech 126:633-640
Yang X (2014) Nature-inspired optimization algorithms. Elsevier Insights, London, UK